Journal of Physics: Conference Series **706** (2016) 052038 doi:10.1088/1742-6596/706/5/052038

Heavy-Quarkonium Potential from Lattice Gluon Propagator

W M Serenone, A Cucchieri and T Mendes

Instituto de Física de São Carlos, Universidade de São Paulo
Caixa Postal 369, CEP 13560-970, São Carlos SP, Brazil

E-mail: willian.serenone@usp.br

Abstract. The study of heavy quarks is of great interest for the search of physics beyond the Standard Model and the understanding of nonperturbative aspects of QCD. One of the early attempts to study these systems was the potential model approach. The Cornell potential is perhaps the most successful of these potentials. However, the use of perturbation theory in its building process implies that it is unable to model confinement without the *ad-hoc* addition of a linear term. In this paper, we modify the Cornell potential by using a (nonperturbative) lattice gluon propagator. This approach allowed us to verify that the use of perturbation theory washes away confinement. We were able to use this modified potential in the Schrödinger equation to obtain numerically the spectrum of heavy quarkonia (charmonium and bottomonium). We use the Cornell-potential spectrum as a benchmark of our potential. The result shows that our potential was able to describe better the spin-average of the experimental states than the Cornell potential. We also computed interquark distances for the quarkonia states.

1. Introduction

After the J/Ψ discovery, its non-relativistic character become evident and the idea of describing heavy quarkonia with potential models was proposed [1, 2]. One of the first proposed models was the Cornell potential. It is to date very popular, due to its simplicity and yet good description of the spectrum. Corroborating it, one can fit it to lattice calculations of the potential between static quarks [3].

The Cornell potential is characterized by the sum of two terms

$$V = -\frac{4}{3}\frac{\alpha_s}{r} + \sigma r\,. \tag{1}$$

The first term resembles the Coulomb potential from electromagnetism, the most notable difference being the 4/3 factor, called "color factor". The similarity of this term with the Coulomb potential is not a coincidence, since its derivation is done by the Fourier transform of the scattering amplitude computed perturbatively — the same process that one can use to derive the Coulomb potential. The second term is added in an "*ad-hoc*" way to reproduce confinement. The motivation for it comes from discretizing QCD on the lattice and computing the Wilson loop in the strong-coupling limit. Also, lattice data support this shape as well, as seen in [3, 4, 5].

The derivation of the Cornell potential uses the free-gluon propagator, thus it is natural to investigate the effects of using a non-perturbative one. Our choice was to use the propagator from Ref. [6], which was obtained by simulating a pure gauge theory with $SU(2)$ symmetry in

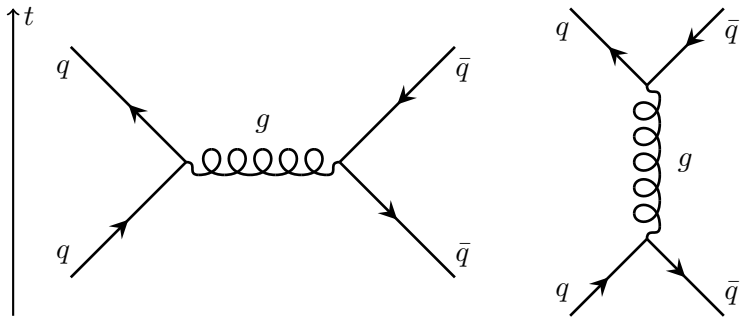

Figure 1. Feynman graph contributing at tree-level to the scattering amplitude T_{fi}. The diagram on the left is a gluon exchange and the one on the right is the brief annihilation of quarks. The latter yields a null contribution to T_{fi}.

Landau gauge. We normalized the propagator so that it would match the perturbative one in the limit $k^2 \to \infty$. We found that it shares the general shape of the Coulomb-like term of the Cornell potential, but presenting some additional features. It is still a non-confining potential and thus needs the addition of the linear term.

Both models have as free parameters the quark masses (m_c and m_b) and the string force σ. We fit these parameters to the spin-averaged spectrum of charmonium and bottomonium. Doing so gives us a way to decide if the obtained potential is indeed an improvement over the Cornell potential. The method allowed us to obtain the wave functions as well and thus we provide estimates of the average particle diameters. This information may be useful to Effective Field Theories, such as potential Non-Relativistic QCD (pNRQCD) [7].

Preliminary results were presented in Refs. [8, 9]. A more complete study can be found in [10].

2. Potential from Lattice Gluon Propagator

For completeness, we will briefly review the method to obtain the Cornell potential. A more detailed review on the subject can be found in Ref. [11].

The scattering-matrix S_{fi} can be expressed, in a first-order approximation, as

$$S_{fi} \equiv \langle f|i\rangle = \delta_{fi} + i(2\pi)^4\,\delta^{(4)}(Q-P)\,T_{fi}\,, \tag{2}$$

where Q and P correspond respectively to the final and initial total momentum and T_{fi} is the scattering amplitude. The two Feynman diagrams that contribute to T_{fi} at tree-level are presented in Fig. 1. We assume that the propagator will be of the form $P^{ab}_{\mu\nu}(k^2) = \delta^{ab} D_{\mu\nu}(k^2)$ and impose that the quark color-state is given by

$$c_q = \frac{(|r\rangle + |g\rangle + |b\rangle)}{\sqrt{3}}\,, \tag{3}$$

while the antiquark is in the color-state $c_{\bar{q}} = c_q^\dagger$. Under these conditions, we obtain that just the left diagram in Fig. 1 actually contributes at tree-level. The same calculation for the remaining term shows that it gets multiplied by a factor 4/3.

In the next step, we impose the non-relativistic approximation $p^2 \ll m^2$, i.e. we drop terms proportional to $1/m^2$. As a consequence, only the component $D_{00}(0, \boldsymbol{k}^2)$ contributes to the scattering amplitude

$$T_{fi} = \frac{4}{3}\frac{g_0^2}{(2\pi)^6} D_{00}(\boldsymbol{k}^2)\,. \tag{4}$$

The potential is then obtained by performing the Fourier transform

$$V(\boldsymbol{r}) = -(2\pi)^3 \int \exp(-i\boldsymbol{k}\cdot\boldsymbol{r})\; T_{fi}(\boldsymbol{k}^2)\, d^3k = -\frac{4}{3}\frac{g_0^2}{(2\pi)^3}\int \exp(-i\boldsymbol{k}\cdot\boldsymbol{r})\; D_{00}(0,\boldsymbol{k}^2)\, d^3k\,. \tag{5}$$

When we choose the free-gluon propagator $D_{\mu\nu}(k^2) = -g_{\mu\nu}/k^2$, Eq. (5) results in the Coulomb-like term of the Cornell potential

$$V(\boldsymbol{r}) = -\frac{4}{3}\frac{\alpha_s}{r}\,, \tag{6}$$

where $\alpha_s = g_0^2/(4\pi)$. As said in Section 1, the linear term is added in an *ad-hoc* way, motivated by lattice computations of the Wilson loop, both numerical [3, 4, 5] and analytical (by expanding e^{-S} in the strong limit coupling [12]).

2.1. Gluon Propagator from Lattice Simulations

In our work, we redo the calculation above using a propagator computed non-perturbatively, using a lattice simulation of a pure SU(2) gauge theory in Landau gauge. It is given by (see Ref. [6, 13, 14])

$$\begin{aligned} P^{ab}_{\mu\nu}(k) &= \frac{C\,(s+k^2)}{t^2+u^2k^2+k^4}\left(\delta_{\mu\nu}-\frac{k_\mu k_\nu}{k^2}\right)\delta^{ab}\,, \\ C &= 0.784, \qquad s = 2.508\,\mathrm{GeV}^2\,, \\ u &= 0.768\,\mathrm{GeV}, \quad t = 0.720\,\mathrm{GeV}^2\,. \end{aligned} \tag{7}$$

Although the simulated theory has $SU(2)$ gauge symmetry, we expect that the only difference with the $SU(3)$ case will be a multiplicative constant [15]. We adjust the multiplicative constant C by requiring that, in the limit $k^2 \to \infty$, the propagator in Eq. (7) behaves like the perturbative one, i.e. $D_{\mu\nu} \sim 1/k^2$. In the non-relativistic approximation, the energy carried by the exchanged gluon is approximately zero ($k_0 \cong 0$) and therefore the contribution of the term $k_\mu k_\nu/k^2$ to the component D_{00} can be neglected. Lastly, we rotate from Euclidean space to Minkwoski space by performing the substitution $\delta_{\mu\nu} \to -g_{\mu\nu}$.

After the above considerations, we insert T_{fi} in Eq. (5) to obtain the potential

$$V(\boldsymbol{r}) = -\frac{4}{3}\,\frac{g_0^2}{(2\pi)^3}\int \frac{C\,(s+\boldsymbol{k}^2)e^{-i\boldsymbol{k}\cdot\boldsymbol{r}}}{t^2+u^2\boldsymbol{k}^2+\boldsymbol{k}^4}\,d^3k = -\frac{4}{3}\,\frac{g_0^2 C}{2i(2\pi)^2 r}\int_{-\infty}^{\infty}\frac{(s+k^2)\left(e^{ikr}-e^{-ikr}\right)}{t^2+u^2k^2+k^4}k\,dk\,, \tag{8}$$

where we already performed the trivial angular integration. The remaining integral can be evaluated using residues. More precisely, we have one simple pole in each quadrant of the complex plane, distributed symmetrically. We consider a semicircular contour closed above (below) to integrate the first (last) term. The result is a sum of four terms (one for each pole). However, since the poles are symmetrically distributed, it is possible to relate the four poles by complex conjugations and changes in signal. This allows us to write the Lattice-Gluon-Propagator potential (V_{LGP}) as

$$V_{LGP}(r) = -\frac{4}{3}\frac{2\alpha_s}{r}\Re\left[\frac{C(s+k_{0,0}^2)\,e^{ik_{0,0}r}}{u^2+2k_{0,0}^2}\right]\,, \tag{9}$$

where

$$k_{0,0} = i\sqrt{t}\,\exp\left[i\,\frac{\theta}{2}\right]. \tag{10}$$

Both V_{LGP} and the Cornell potential depend on the strong coupling constant α_s. As it is known, the QCD coupling has a dependence on the energy scale of the process. We use as the energy scale the mass of the 1S state of the system considered [J/ψ for charmonium and $\Upsilon(1S)$ for bottomonium]. Ref. [16, Section 9] presents us with with the four-loop calculation for α_s as well as values for Λ_{QCD}, which we use in computing the two different values of α_s.

The result in Eq. (9) is a non-confining potential, just as in the Cornell-potential case. But we notice that it contains qualitative differences from the Coulomb-like one. For instance, it does rise above zero, showing a behavior that would be expected for a confining potential until around 1.5 fm. After this region, the potential is damped. For the calculation of the eigenstates (see Section 3), we thus add a linear term σr to model confinement, as it is done for the Cornell potential

$$V_{LGP+L}(r) = V_{LGP}(r) + \sigma r\,. \tag{11}$$

3. Finding Eigenstates and Fitting

The V_{LGP+L} and the Cornell potential are very similar and thus it is expected that V_{LGP+L} will yield a spectrum similar to the Cornell potential, but perhaps with an improved description of the bound-state energies. Since we are in a non-relativistic regime, it is possible to perform this check by solving the Schrödinger equation. We perform the usual variable separation, i.e. the wave function is given by[1] $\psi^m_{l,n}(\boldsymbol{r}) = f_n(r)Y^m_l(\theta,\varphi)/r$. The function $f_n(r)$ has to obey the boundary conditions $f_n(0) = 0$ and $f_n(r \to \infty) = 0$. Due to the complexity of the potentials involved, we choose to solve the ordinary differential equation for $f_n(r)$ numerically.

For the numerical solution, we use the *shooting method* [17]. It consists in discretizing a likely range to find the eigenenergies and, for each one of these points, we compute the wave function. We know that the boundary conditions will only be met for the exact value of the eigenenergy. Therefore, if we determine the energy value for which the wave function most closely matches the boundary conditions, we know that this energy will be a good approximation for an eigenenergy.

The way we implement the strategy above is to start the integration of $f_n(r)$ for a large value of r, where we can consider only the linearly rising term of the potential. In this regime, we know that the solution will be an Airy function of the first kind and thus we have analytic values for the initial point and its derivative. We integrate towards $r = 0$ using a second-order Runge-Kutta method (more precise methods showed little improvements). If we compare the value of $f_n(0)$ for two consecutive energies and find that it changed sign, we know that the eigenenergy must be inside the range delimited by these energies. We then adapt the bisection method to further refine the precision of the found eigenenergy.

We remark that our model has as free parameters the charm and bottom quark mass (m_c and m_b) as well as the string force σ. To fit the eigenenergies obtained numerically, to the experimental spectrum, we set up a grid of points m_c, m_b and σ and compute the spectrum for each one of the points. It is then possible to compute the χ^2 value

$$\chi^2(m_c,\, m_b,\, \sigma) = \sum_i \left(\frac{E_i - E_{i,\text{experimental}}}{\sigma_i}\right)^2 \tag{12}$$

and select the parameters that minimize it. We also compute the uncertainty associated with this calculation by delimiting the area for which the χ^2 rises by no more than one unit. The errors in the parameters are then obtained by projecting the area on the parameter axis. We propagate these errors to the spectrum by generating random numbers around the central values of the fit, following a Gaussian distribution with standard deviation equal to the established errors.

The experimental states found are spin dependent, while our spectrum is not. Therefore, we average over states with same angular momentum and principal quantum number, but different

[1] We notice that the potential in Eq. (11) is central.

Figure 2. The charmonium spectrum obtained using V_{LGP+L} and the Cornell potential, along a comparison with the spin-averaged states.

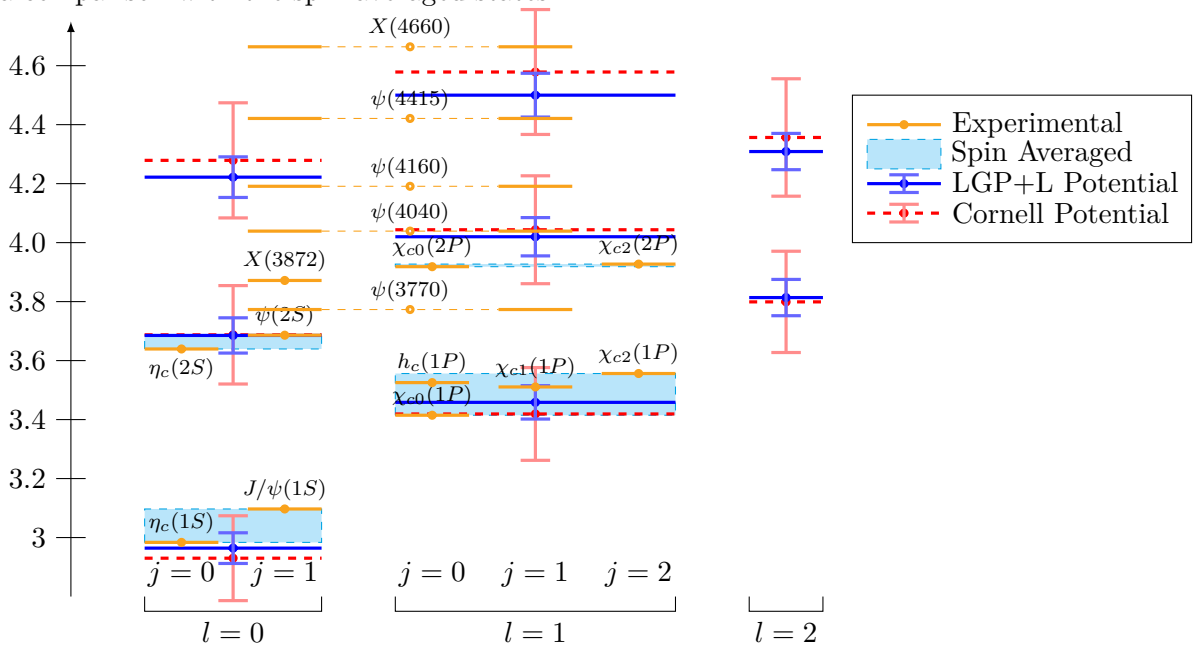

spins. Our choice was to simply take the average of the minimum and maximum values of mass for each case and assign the uncertainty σ_i as half the distance between them. The values were extracted from Ref. [16].

4. Results

The numerical results below were obtained using the following parameters: The wave function was integrated from $r = 20.0\,\mathrm{GeV}^{-1}$ until the origin (as described in the Section 3) in steps of $5.0 \times 10^{-3}\,\mathrm{GeV}^{-1}$. We searched the charm quark mass in the range between 1.00 GeV and 2.00 GeV in steps of 1×10^{-3} GeV. The search for the bottom quark mass used the same step, but in the range between 4.15 GeV and 4.85 GeV. The last parameter, i.e. the string force σ, is searched in the range from $0.10\,\mathrm{GeV}^2$ to $0.50\,\mathrm{GeV}^2$ in steps of $0.01\,\mathrm{GeV}^2$. We used $\alpha_s = 0.2663$ when solving the differential equation for charmonium and $\alpha_s = 0.1843$ for bottomonium. Lastly, we present the discretization used in the search for eigenenergies. For simplicity, our search was made for the total particle mass (by replacing in the differential equation the eigenenergy with $M_{\mathrm{Tot}} - 2m_q$). For the charmonium, we searched for masses between 2.00 GeV and 6.00 GeV in steps of 0.04 GeV. For the bottomonium, we searched from 8.50 GeV until 12.50 GeV using the same step as for charmonium.

The spectrum obtained with both potentials can be found in Tables 1 and 2 as well in Figures 2 and 3. The parameters that minimized χ^2 can be found in Table 3. As it is possible to see from these tables and figures, the spectrum obtained from V_{LGP+L} is similar to the one from the Cornell potential, as expected. But we must point out that V_{LGP+L} shows a small but observable improvement over the Cornell potential. This can also be seen by the smaller value of χ^2 obtained from the fit. We notice as well that the error associated to each state in the spectrum is smaller in the V_{LGP+L} case. We can see in Table 3 that we are able to determine the model parameters more precisely for the V_{LGP+L} as well.

As described in Section 3, the process of determining the spectrum goes through finding the wave function. The raw output yields non-normalized wave functions. We normalize them and

Table 1. Results for the charmonium eigenstates using V_{LGP+L} and the Cornell potential.

V_{LGP+L}			Cornell Potential		
State	Predicted mass (GeV)	Deviation from averaged spin (GeV)	State	Predicted mass (GeV)	Deviation from averaged spin (GeV)
1S	2.96(5)	−0.10	1S	2.93(14)	−0.14
2S	3.69(6)	0.01	2S	3.69(17)	0.01
3S	4.22(7)	-	3S	4.28(20)	-
1P	3.46(6)	−0.07	1P	3.42(16)	−0.11
2P	4.02(6)	0.09	2P	4.04(18)	0.12
3P	4.50(7)	-	3P	4.58(21)	-
1D	3.81(6)	-	1D	3.80(17)	-
2D	4.31(6)	-	2D	4.36(20)	-

Table 2. Results for the bottomonium eigenstates using V_{LGP+L} and the Cornell potential.

V_{LGP+L}			Cornell Potential		
State	Predicted mass (GeV)	Deviation from averaged spin (GeV)	State	Predicted mass (GeV)	Deviation from averaged spin (GeV)
1S	9.47(4)	0.04	1S	9.49(8)	0.06
2S	10.00(4)	−0.01	2S	10.00(10)	−0.01
3S	10.37(5)	0.01	3S	10.39(12)	0.03
4S	10.67(6)	0.10	4S	10.72(14)	0.14
5S	10.95(7)	-	5S	11.01(16)	-
1P	9.86(4)	−0.03	1P	9.84(10)	−0.04
2P	10.24(5)	−0.01	2P	10.25(11)	0.00
3P	10.56(5)	0.03	3P	10.59(13)	0.05
4P	10.84(6)	-	4P	10.89(15)	-
1D	10.11(5)	−0.05	1D	10.10(11)	−0.06
2D	10.44(5)	-	2D	10.45(12)	-
3D	10.73(6)	-	3D	10.77(14)	-

Table 3. Quark masses and string tension obtained from our fit. These parameters are used to obtain the spectrum in Tables 1 and 2.

V_{LGP+L}	Cornell Potential	Quark Mass in Ref. [16]
$m_c = 1.16(3)\,\text{GeV}$	$m_c = 1.11^{+0.08}_{-0.02}\,\text{GeV}$	$m_c = 1.275(25)\,\text{GeV}$
$m_b = 4.61^{+0.02}_{-0.01}\,\text{GeV}$	$m_b = 4.58^{+0.04}_{-0.01}\,\text{GeV}$	$m_b(\overline{MS}) = 4.18(3)\,\text{GeV}$
$\sigma = 0.23(1)\,\text{GeV}$	$\sigma = 0.26^{+0.01}_{-0.03}\,\text{GeV}$	$m_b(1S) = 4.66(3)\,\text{GeV}$
$\chi^2 = 6.20$	$\chi^2 = 12.13$	

Figure 3. The bottomonium spectrum obtained using V_{LGP+L} and the Cornell potential, along a comparison with the spin-averaged states.

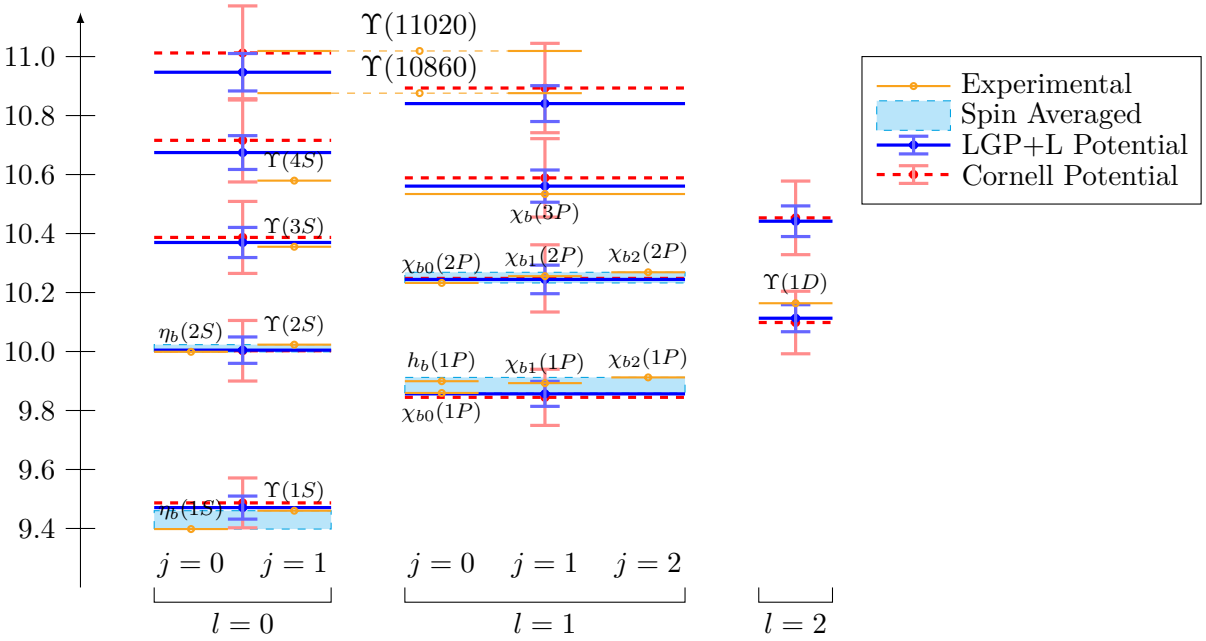

Table 4. Typical inter-quark distances for charmonium and bottomonium. Errors are expected to be negligible.

Charmonium			Bottomonium		
State	V_{LGP+L} distance (fm)	Cornell Potential distance (fm)	State	V_{LGP+L} distance (fm)	Cornell Potential distance (fm)
1S	0.80	0.83	1S	0.45	0.47
2S	1.59	1.56	2S	0.94	0.94
3S	2.20	2.14	3S	1.35	1.31
1P	1.29	1.28	1P	0.76	0.77
2P	1.94	1.90	2P	1.18	1.16
3P	2.50	2.43	3P	1.55	1.49

compute the mean diameter of particles

$$\langle d \rangle = 2 \int_0^\infty |f(r)|^2 \, dr \, . \tag{13}$$

The results are found in Table 4. These results may be useful in Effective Field Theories, such as pNRQCD [7].

5. Summary

In this work we employed a potential model for heavy-quarkonia states using a non-perturbative potential obtained through lattice simulations. We found that the potential is still non-confining, which is expected, since perturbation theory is employed for its derivation. Despite this, we find that it shows small qualitative differences from the Coulomb-like term of Cornell potential. The most interesting one is that it rises above zero, showing a behavior similar

to the one expected for a confining potential up to around $\sim 1.5\,\mathrm{fm}$. It is damped however for larger distances.

We proceeded to compute the spectrum using the Cornell and V_{LGP+L} for charmonium and bottomonium. The results showed that the corrections introduced in V_{LGP+L} through the use of the lattice gluon propagator improved the spectrum and narrowed the errors. Our interpretation is that the propagator in Eq. (7) contains information about QCD that is missing from the free propagator, even in the perturbative regime. We also obtained the wave functions of the quarkonia states and were able to compute the mean diameter of such states, which may be useful to pNRQCD [7].

Acknowledgments

The authors thank B. Blossier and F. Navarra for useful comments. W.S. thanks the Brazilian funding agencies FAPESP and CNPq for financial support. A.C. and T.M. thank CNPq for partial support. For drawing Fig. 1, we used the `feynman` LaTeXpackage available at `http://feynman.aivazis.com/`.

References

[1] Eichten E, Gottfried K, Kinoshita T, Lane K D and Yan T M 1978 *Phys. Rev.* D **17** 3090 [Erratum: Phys. Rev.D21,313(1980)]
[2] Eichten E, Gottfried K, Kinoshita T, Lane K D and Yan T M 1980 *Phys. Rev.* D **21** 203
[3] Bali G S 2001 *Phys. Rept.* **343** 1–136 (*Preprint* `hep-ph/0001312`)
[4] Koma Y, Koma M and Wittig H 2006 *Phys. Rev. Lett.* **97** 122003 (*Preprint* `hep-lat/0607009`)
[5] Koma M, Koma Y and Wittig H 2008 *PoS* **CONFINEMENT8** 105
[6] Cucchieri A, Dudal D, Mendes T and Vandersickel N 2012 *Phys. Rev.* D **85** 094513 (*Preprint* `1111.2327`)
[7] Brambilla N *et al.* 2014 *Eur. Phys. J.* C **74** 2981 (*Preprint* `1404.3723`)
[8] Serenone W M and Mendes T 2013 *AIP Conf. Proc.* **1520** 364–366
[9] Serenone W M, Cucchieri A and Mendes T 2014 *PoS* **LATTICE2013** 434 (*Preprint* `1404.7436`)
[10] Serenone W M, Cucchieri A and Mendes T 2015 (*Preprint* `1505.06720`)
[11] Lucha W, Schoberl F F and Gromes D 1991 *Phys. Rept.* **200** 127–240
[12] Creutz M 1983 *Quarks, Gluons and Lattices* Cambridge Monographs on Mathematical Physics (Cambridge University Press) ISBN 9780521315357
[13] Cucchieri A and Mendes T 2007 *PoS* **LAT2007** 297 (*Preprint* `0710.0412`)
[14] Cucchieri A and Mendes T 2008 *Phys. Rev. Lett.* **100** 241601 (*Preprint* `0712.3517`)
[15] Cucchieri A, Mendes T, Oliveira O and Silva P J 2007 *Phys. Rev.* D **76** 114507 (*Preprint* `0705.3367`)
[16] Olive K A *et al.* (Particle Data Group) 2014 *Chin. Phys.* C **38** 090001
[17] Press W H, Teukolsky S A, Vetterling W T and Flannery B P 2007 *Numerical Recipes 3rd Edition: The Art of Scientific Computing* (Cambridge University Press) ISBN 9780521880688